

Boomitra's MRV Framework for Monitoring Soil Carbon in Indian Smallholder Farms (URVARA Project)

A transparent, science-based overview of our satellite- and AI-enabled soil carbon measurement system, designed for cost-effective precision and broad smallholder inclusion—featuring detailed methods, calibration data, uncertainty quantification, and validation results.



Table of Contents

INTRODUCTION: BOOMITRA’S MRV FRAMEWORK FOR INDIAN SMALLHOLDER FARMS IN OUR URVARA PROJECT	3
SECTION 1: OVERALL MRV PROCESS FLOW	3
SECTION 2: THE SCIENCE BEHIND REMOTE SENSING OF SOC.....	4
2.1 PHYSICAL PRINCIPLES OF SOC ESTIMATION USING REMOTE SENSING	4
2.2 MODEL CALIBRATION DATASET FOR INDIAN CROPLANDS.....	7
2.3 MODEL VALIDATION DATASETS.....	10
2.4 SATELLITE COVARIATES	10
2.5 MODEL CALIBRATION	11
2.6 MODEL VALIDATION METRICS.....	13
SECTION 3: UNCERTAINTY QUANTIFICATION	15
3.1 SOURCES OF UNCERTAINTY	15
3.2 BAYESIAN APPROACH TO UNCERTAINTY QUANTIFICATION	17
SECTION 4: QUANTIFICATION OF NET CARBON REMOVALS	18
SECTION 5: DISCUSSION AND LIMITATIONS	21
5.1 INTERPRETING THE SEQUESTRATION RESULTS IN CONTEXT	21
5.2 MODEL STRENGTHS AND PRACTICAL VALUE	23
5.3 LIMITATIONS AND CONSIDERATIONS.....	23
5.4 ROBUSTNESS IN REVERSAL MONITORING	24
5.5 ADVANTAGES OF EX-POST CREDIT ISSUANCE	24
5.6 REMOTE SENSING FOR HIGH-QUALITY, SCALABLE MRV	24
APPENDIX A: READER QUESTIONS AND RESPONSES	25

Introduction: Boomitra's MRV Framework for Indian Smallholder Farms in our URVARA Project

Boomitra is committed to delivering inclusive, scientifically rigorous carbon projects. A core challenge in soil organic carbon (SOC) monitoring is the cost of traditional sampling at the resolution required to track changes at the individual smallholder farm level. For robust project-scale measurement, each farm typically requires at least one soil sample—often more. This quickly becomes cost-prohibitive given the current economics of carbon credit pricing.

Even in India—where lab costs are among the lowest globally (\$10–\$20 per sample for testing alone, excluding field collection)—sampling remains economically infeasible for smallholders. SOC sequestration rates from regenerative practices in these systems typically range between 0.2 and 0.7 tC/ha/year (0.7–2.6 tCO₂e/ha/year or 0.004–0.014 wt%/year)¹. At prevailing carbon credit prices (~\$15/tCO₂e at the time of writing²), the expected credit revenue per hectare is often insufficient to justify full-scope sampling. In the best-case scenario, sampling and testing might consume ~25% of revenue per hectare. In the worst case, they exceed the value of the credits altogether. These figures exclude further project costs related to auditing, registration, and ongoing MRV.

To overcome this barrier, Boomitra has developed a remote sensing-based soil carbon monitoring system that is both cost-effective and scientifically robust. Certified under the Social Carbon Standard, this approach pairs satellite-based microwave and VIS-IR imagery with localized ground-truth data and machine learning. The result is a scalable MRV system capable of measuring SOC change across thousands of smallholder farms while maintaining measurement fidelity.

The system integrates: Microwave backscatter, which probes the soil's dielectric properties at depth, and VIS-IR satellite data, which captures surface vegetation signals relevant to improving soil modeling.

Together, these inputs enable accurate estimation of SOC changes across India's tropical and subtropical agricultural landscapes. The measurement framework has undergone detailed evaluation as part of validation and verification audits under the Social Carbon Standard, including peer-review by independent experts in soil science and remote sensing. Furthermore, the framework has taken inputs from Boomitra's other registered projects under Verra's VCS Standard, ensuring compatibility across leading standards in the carbon markets.

The following sections outline the complete MRV process—from physical principles and model calibration through to uncertainty quantification and project-level crediting—providing transparency for technical reviewers, credit buyers, and stakeholders.

We invite you to submit comments and questions on this work using [this form](#). All submissions will be reviewed and addressed, and both the questions/comments and our responses will be appended to the end of this document for reference and transparency.

Section 1: Overall MRV Process Flow

The MRV process follows a structured approach, integrating satellite data, ground-truth measurements, and modeling techniques, following the overarching guidance of the [Social Carbon SCM5 methodology](#):

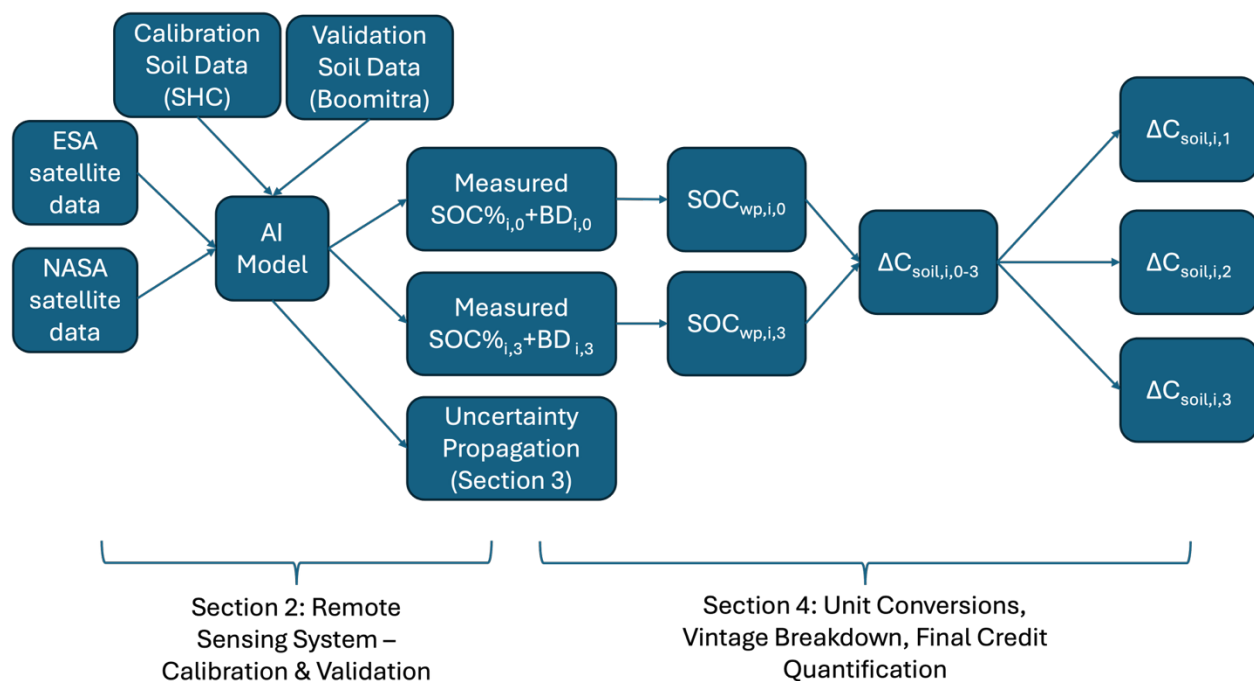


Figure 1. Overall MRV Process

The MRV process consists of:

1. The remote sensing and AI system to measure SOC and bulk density at the pixel-level, which is the subject of Section 2.
2. The associated uncertainty propagation to robustly account for all sources of error in our calculations, which is the subject of Section 3.
3. The necessary unit conversions to get to the soil carbon stock change, and methodology equations to calculate the total credits and their vintage breakdown, which is described in Section 4.

This article wraps-up with a discussion of the results across the first set of farms in the project (Section 5).

Section 2: The Science Behind Remote Sensing of SOC

2.1 Physical Principles of SOC Estimation Using Remote Sensing

Accurately estimating SOC at scale requires bridging the gap between physical soil properties, remote sensing signals, and predictive modeling. This section outlines the scientific principles underlying Boomitra's approach, including the role of microwave interactions with soil, the influence of soil structure and composition on the dielectric response, and the use of machine learning models to translate remote measurements into reliable SOC stock estimates.

The foundation of Boomitra's SOC monitoring lies in established scientific principles combined with the latest remote sensing and machine learning techniques. The technology leverages satellite-based microwave remote sensing, particularly in the L- and P-bands, where longer wavelengths on the order of several centimeters can penetrate thin vegetation cover and probe the soil beneath³.

The depth to which microwaves can penetrate into the soil depends on the microwave wavelength and the soil's dielectric properties. Under low soil moisture conditions, the effective sensing depth can extend beyond 30 cm for L-band and up to 80 cm for P-band microwaves³. Measuring the soil dielectric constant using microwave remote sensing is a well-established method for calculating soil moisture, as increasing moisture significantly raises the dielectric constant, thereby increasing the microwave energy scattered back from the soil⁴.

However, the soil dielectric constant (ϵ_r) is influenced by more than just moisture. It can be understood as a volumetric weighted average of the soil's solid, liquid, and gaseous components, expressed as⁵:

$$\epsilon_r = (1 - \phi)\epsilon_{r,s} + \theta\epsilon_{r,l} + (\phi - \theta)\epsilon_{r,g}$$

where,

- $\epsilon_{r,s}$ is the solid-phase dielectric constant, made up of a volumetric weighted sum of the dielectric constants of the mineral particles (sand, silt, clay) and soil organic matter (SOM).
- $\epsilon_{r,l}$ is the liquid-phase dielectric constant, corresponding to moisture (water, $\epsilon_{r,H_2O} = 78.4$).
- $\epsilon_{r,g}$ is the gaseous-phase dielectric, corresponding to air (atmosphere, $\epsilon_{r,atm} = 1.0006$).
- θ is the volumetric soil moisture content (vol% or %v/v).
- ϕ is the soil porosity (vol% or %v/v), representing the fraction of the soil volume not occupied by solids (e.g., sand, silt, clay, organic matter).

Among the solid components, while soil texture tends to remain relatively constant over time at a given location, SOM levels can vary significantly. The dielectric constants of sand, silt, clay, and SOM typically range between 2 and 10, depending on the soil's mineral origin⁶. Importantly, SOM generally exhibits a lower dielectric constant than mineral particles⁶. Therefore, an increase in SOM content tends to reduce the solid-phase dielectric constant $\epsilon_{r,s}$, which in turn influences the overall soil dielectric behavior detectable by remote sensing.

Porosity, a key descriptor of soil structure linked inversely to bulk density (BD), arises from the interplay of soil texture, SOM, and the soil's compaction history (e.g., from heavy equipment or livestock). An increase in SOM typically enhances porosity. Empirical studies confirm that both porosity and moisture are crucial factors influencing the soil dielectric⁷.

Therefore, when soil texture, soil moisture, and compaction history are accounted for, SOC can be determined from the dielectric constant, through its effects on decreasing $\epsilon_{r,s}$ and increasing porosity, which both collectively decrease the dielectric constant, leading to a diminished microwave backscatter.

At the same time, the above ground vegetation can also have an effect on microwave backscatter. The effect is much smaller for crops than for forests, because their cross-sectional area is much smaller with respect to microwave wavelengths. Dense forests can prevent the microwave signal from reaching the soil, and are thus out of scope for this work. On the other hand, for most cropping systems, the effect is primarily a slight attenuation of the like-polarized radar backscatter⁸. This has allowed for algorithms using microwave satellite data to measure soil moisture, a measurement that is routinely used in weather prediction systems today⁹.

Extensive literature has shown that crops can be well-measured through multispectral satellite data¹⁰. Thus, to effectively disentangle the contributions of vegetation and soil to the microwave signal and to learn the complex empirical relationship between the measured soil dielectric and SOC, Boomitra employs a machine learning (ML) model that fuses data from various spectral ranges, including visible, infrared, and microwave bands.

Furthermore, when soil texture and compaction history are known and considered constant, BD and SOC often exhibit an inverse correlation. This relationship can be captured by a region-specific pedotransfer function (PTF)¹¹, allowing BD—and subsequently, the total soil carbon stock in tons per hectare—to be estimated once SOC, soil texture, and compaction are known. Note that soil texture is stable over human timescales at a given location, and compaction history can be determined from activity monitoring at each farm participating in the project. Several PTFs are available in the literature, with varying levels of accuracy, but the most accurate PTFs are those that are very narrow in their scope of use¹¹. For this reason, Boomitra builds custom PTFs with localized calibration soil data in order to reach maximum accuracy for the different soil types within a given project.

Once calibrated, the model can be applied to new locations within its calibration scope (e.g., areas with similar soil type and climatic conditions), using the learned relationship to convert microwave-derived dielectric measurements into SOC estimates. BD is then derived via the PTF, enabling the final soil carbon stock calculation.

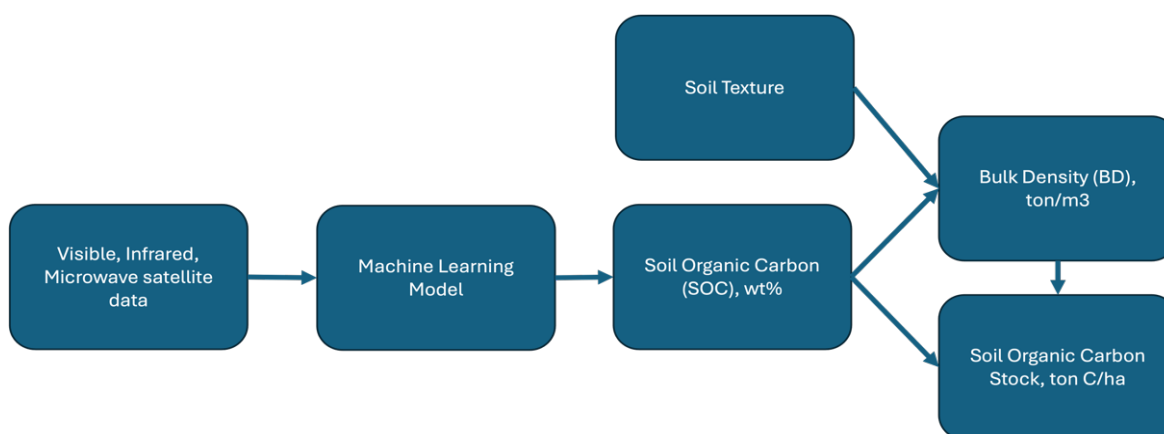
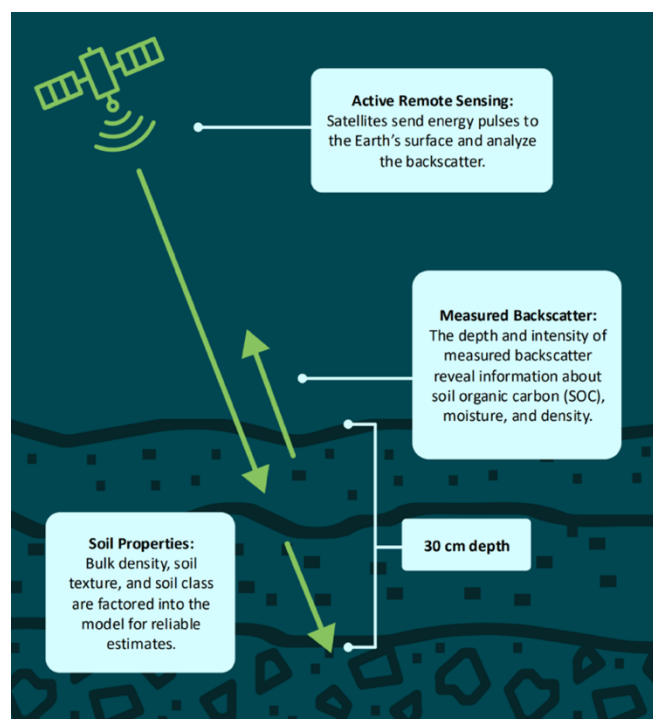


Figure 2. Model prediction process to determine soil organic carbon stock. The measurement of microwave backscatter provides soil dielectric data that is causally related to the SOC (above) and the combination of different data sources through machine learning enables a robust prediction (below). Data sources are described further in the subsequent sections.

Hence, the theoretical basis relies on four assumptions:

1. Microwave backscatter can directly measure the soil dielectric constant (to 30-80cm depth, depending on the wavelength used).
2. Soil dielectric is causally related to SOC, decreasing as SOC increases, when moisture, texture, and compaction history are known.
3. SOC and BD are correlated under constant soil texture and compaction history, allowing a customized PTF to estimate BD from SOC.
4. ML models trained on absolute SOC levels use the space-for-time substitution to track SOC changes over time. This assumes that covariates explaining spatial differences in SOC can also explain temporal changes. This is related to Assumption 2—if Assumption 2 is true and the soil dielectric, and thus microwave backscatter, is causally related to SOC, then it is more plausible for the space-for-time substitution to be applicable. If the model has then learned the same mechanism, it can translate its learnings from spatial variation into temporal variation.

The validity of Assumption 1 is maintained by limiting the scope of this work to only appropriate cropping regions where it is true (eg. no dense tree cover etc.). Assumption 3 is shown to be valid below in the implementation of our project's custom PTFs. Assumptions 2 and 4 have been independently validated through matched-pairs controlled trials across different regions, with results to be published in upcoming peer-reviewed journal articles.

2.2 Model Calibration Dataset for Indian Croplands

The practical implementation of this framework is tested across the diverse croplands of India, which encompass a wide range of cropping systems, from staples like rice and wheat to cash crops such as banana and sugarcane. A variety of regenerative agricultural practices are promoted across the project area, include crop residue retention and reincorporation, organic fertilizer application, crop rotations, cover cropping, and intercropping with legumes. These practices are adapted regionally across the states of Karnataka, Maharashtra, Tamil Nadu, Madhya Pradesh, Andhra Pradesh, and Kerala, reflecting the diverse cropping systems present in the project area. The project currently has 8,000 farms, and the average farm size is 1.2 ha, which is very close to the 1.08 ha average size across the country reported by Indian census data¹².

India experiences distinct wet (monsoon) and dry seasons, which vary regionally¹³. The driest months, typically January to May, are generally ideal for remote sensing-based SOC quantification in rainfed areas, as the confounding effect of soil moisture is minimized. However, with about 55% of Indian farms having access to irrigation¹⁴, SOC measurements for these farms are best taken between cropping seasons (Rabi: Oct-Mar; Kharif: Jun-Oct) when irrigation is off. Therefore, the period from March to May is suitable for irrigated farms as well, lacking both active irrigation and monsoon rains.

The SOC machine learning model calibration relies primarily on ground-truth data from India's extensive Soil Health Card (SHC) program, a government initiative under the National Mission for Sustainable Agriculture (NMSA)¹⁵. This program has generated over 911,712 georeferenced soil samples from 2015 to 2022, analyzed for SOC using the Walkley-Black method, a widely used wet chemistry technique that is the most common SOC testing method in India. Sampling density is

approximately one sample per 2.5 hectares in irrigated areas and one sample per 10 hectares in rainfed areas. Each sample was composited from multiple subsamples within a farm field and analyzed at the nearest district-level NMSA laboratory, typically located at the main Krishi Vigyan Kendra (KVK)—India's governmental agricultural extension network office—within the district. This approach ensures nationwide cropland coverage and adherence to a standardized protocol for collection, processing, testing, and reporting.

The SHC dataset provides SOC (wt%), sample location, and collection date. The dataset's mean SOC is 0.600wt% (standard deviation 0.515wt%, with values generally ranging from 0 to 3wt%) aligning well with independent literature that cites average SOC on Indian farms around 0.7wt%¹⁶. The calibration data undergoes cleaning, primarily restricting SOC values to the 0-3wt% range, which involves removing less than 0.5% of the total samples identified as outliers. This range covers the vast majority of samples, as the distribution count diminishes significantly beyond 1.5wt% (Figure 3).

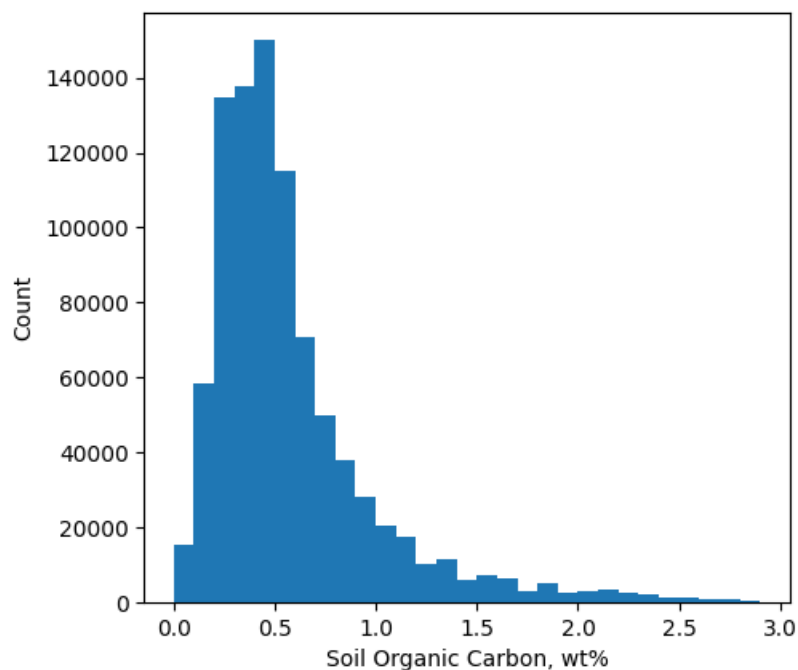


Figure 3. Distribution of SOC in calibration dataset

Although the SHC dataset shows good spatial coverage across most agricultural regions of India (Figure 4), there are parts of the desert regions in north-west India, forested regions in central India, and mountainous sections in the far north and north-east that lack soil sampling. As a result, these areas are outside the model's domain, and precautions are taken to exclude farms located there from the project.

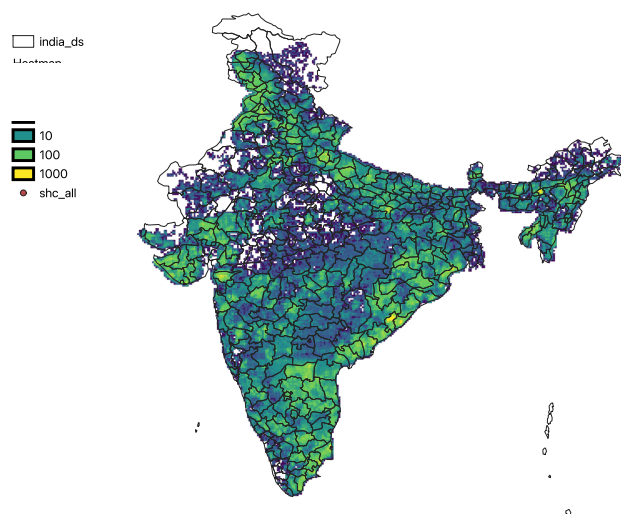


Figure 4. The SHC soil samples (N=911,712) as a spatial heat map by SOC level. Each pixel above is 0.1 x 0.1 degrees and its color represents the number of SOC samples within the pixel

A limitation of the SHC dataset is the absence of BD data, a common issue in many soil surveys. To address this and enable the model to learn the necessary SOC-BD relationships, data from the World Soil Information Service (WoSIS) is utilized¹⁷. WoSIS aggregates global soil data, harmonized through standardized definitions, procedure descriptions, plausibility checks, and units. From WoSIS, approximately 34,000 samples having SOC, BD, and soil texture data, and corresponding to FAO soil types found in Indian croplands, were selected for building the pedotransfer functions.

For consistency with the SOC model training, the WoSIS data used was primarily restricted to samples analyzed using the Walkley-Black method for SOC (about 80% of samples) and sampled to 30cm depth. The WoSIS dataset provides geocoordinates, sampling depths, sampling dates, SOC (wt%), and BD (ton/m³). This careful selection and harmonization process, ensuring consistency in analytical methods (Walkley-Black, expected uncertainty ~0.10wt%) and sampling depth across both SHC and the utilized WoSIS subset, is crucial for building robust models.

The representativeness of these calibration datasets with respect to the project areas' climate zones and soil types is thoroughly assessed and confirmed. The tables below confirm that thousands of calibration samples exist for each key soil type and climate zone combination present in the initial project farms, ensuring adequate representation.

IPCC Climate Zone ^{18*}	Number of Calibration Soil Samples	Number of Project Farms
Tropical Dry	231,488	4,241
Tropical Moist	75,251	2,988
Tropical Wet	41,832	781

FAO Soil Type ^{19*}	Number of Calibration Soil Samples	Number of Project Farms
Acrisol	3,610	1,392
Cambisol	27,108	356
Luvisol	122,570	2,800
Nitrosol	60,171	1,069
Vertisol	47,575	2,393

* The calibration soil samples cover many more soil types and climate zones, but the five soil types and three climate zones given here are the only ones found among the farms currently in the project.

2.3 Model Validation Datasets

Beyond calibration, the project implements ongoing validation through the collection of new soil samples from project farms prior to each verification period. This involves stratified random sampling, with strata defined by FAO soil types¹⁹, selecting approximately 30-50 farms per stratum (determined based on the minimum number of samples conservatively needed to show $R^2 > 0$ for the model, one of the key validation metrics). Composite samples (5-10 subsamples in a zig-zag pattern covering the farm) are collected to 30cm depth and sent refrigerated to a lab within 3 days. These validation samples are tested for SOC using the gold-standard dry combustion method and for BD via oven drying and weighing. For the first verification, 200 such samples were collected in 2024 across the five soil types found within the project's farms (Luvisols, Acrisols, Vertisols, Nitrosols, Cambisols).

To ensure reliable validation results, a rigorous lab selection process was undertaken due to India's large size precluding the use of a single lab. Blind testing was performed using split samples from 15 project farms sent to three private labs (all nationally certified), and ICRISAT (an internationally recognized CGIAR and FAO GLOSOLAN²⁰ regional focal point lab). ICRISAT and two of the labs showed good intra-lab consistency (0.2-0.3wt% variation), while the third private lab exhibited higher variation (>1wt%) and was excluded. Inter-lab comparisons revealed systematic, correctable differences between the remaining three labs, allowing their results to be harmonized using ICRISAT as the benchmark. The 200 validation samples were subsequently tested at these three selected and harmonized labs.

2.4 Satellite Covariates

Satellite data is sourced from multiple platforms to provide comprehensive inputs for the models:

Satellite	Sensor Type	Bands Used	Spatial Resolution	Revisit Time	Availability	Region	Source	Pre-Processing
Sentinel-2	Multi-Spectral	Visible (Bands 1-4); Red-Edge (Bands 5-7, 8a) Near Infrared (Band 8); Short Wave Infrared (Bands 10-12); Water Vapor (Band 9)	10m (Bands 2, 3, 4, 8); 20m (Bands 5, 6, 7, 8a, 11, 12); 60m (Bands 1, 9, 10)	5 days	2016-Present	Global	ESA	The Copernicus Data Store Level-2A product ²¹ is used, which has all bands atmospherically corrected to surface reflectance.
ALOS-2	SAR	L-Band: HH (like-polarized); HV (cross-polarized); Incidence Angle	25m	1 year	2014-Present	Global	JAXA ²²	The SAR Mosaic product ²³ is used, which has undergone the conventional SAR-specific corrections: orbit corrections, orthorectification, radiometric slope corrections, and conversion to gamma0, as detailed in the dataset description
SMAP ²⁴	Radiometer	L-Band: processed to soil moisture	9km	2-3 days	2015-Present	Global	NASA ASF/ ESA CDS	The "Combined" satellite soil moisture product provided by the Climate Data Store (CDS) ²⁵ , which has processed to radiometer data to a volumetric soil moisture level (% v/v)
SMOS ²⁶	Radiometer	Same as SMAP	40km	3 days	2009-Present	Global	ESA CDS	Same as SMAP

A consistent 10m x 10m pixel size is used for analysis, matching Sentinel-2's native resolution in the visible spectrum; ALOS-2 data and other Sentinel-2 bands are downsampled using bicubic interpolation, while the coarser SMAP/SMOS data is used without resampling. Each 10m pixel represents 1/100th of a hectare. For each ground sample location, satellite data is extracted from the overlapping pixel. L-Band SAR data (ALOS or ALOS-2) is chosen based on the image date closest to the soil sample date. Corresponding Sentinel-2 data is then selected, prioritizing the cloud-free and shadow-free pixel closest in time to the SAR image, using ESA's 'sen2cor' tool for masking. Radiometer-derived soil moisture data is collected for the date matching the chosen ALOS SAR image. Data retrieval is automated using Python scripts. The satellites used (from NASA, JAXA, ESA) have long-term operational support, ensuring data continuity for the project's duration. Specific satellite image IDs used for each farm's soil carbon calculations are archived internally, to allow for reproducibility.

2.5 Model Calibration

The initial training of the SOC model involves segmenting the calibration data by FAO soil type, recognizing that soil texture significantly influences the relationship between satellite data and SOC. For each soil type present in the project (Luvisols, Acrisols, Nitosols, Vertisols, and Cambisols at first verification), a separate Random Forest (RF) ensemble model is trained using the scikit-learn library in Python. RF is a well-established algorithm that has shown success in various remote sensing applications, and it was chosen after trying several different regression algorithms (support vectors,

neural nets, kernel ridge regression, gradient boosting etc.) to minimize test RMSE. All mined satellite bands (15 covariates total) are used directly as inputs to the RF. A 90-10 train-test split is employed. Model hyperparameters, such as the number of estimators and tree depth (e.g., 700 estimators, depth 1 for Luvisols), were optimized through trial and error. The performance for the most prevalent soil type, Luvisols (covering 35% of project farms), shows the model's calibration on training ($n=110,313$) and testing ($n=12,257$) data from the SHC dataset (2015-2021).

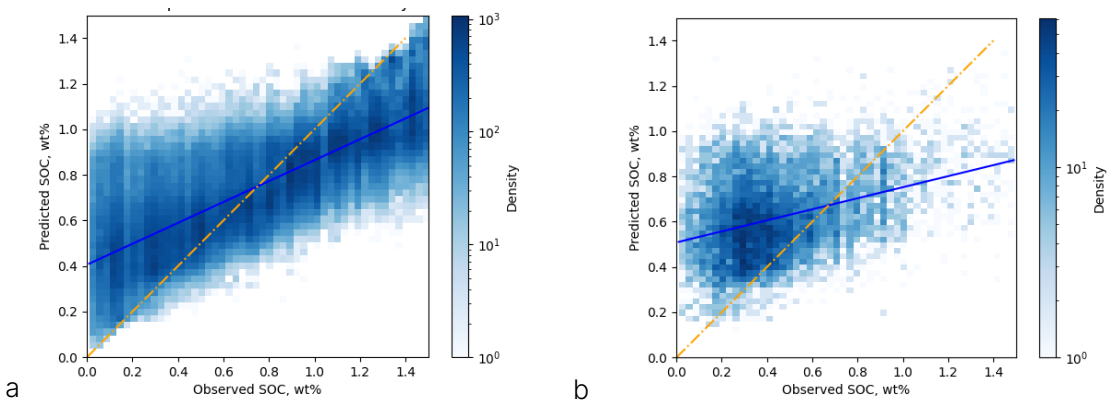


Figure 5. Calibration of the ML model for the remote sensing of SOC. The performance on the train data ($n=110,313$ farms sampled) (a) and test data ($n=12,257$ farms sampled) (b) is shown using the SHC calibration dataset (years 2015-2021) for India, as heatmaps. Summary statistics are in the table below. Due to the large N , the observed slopes of observed vs predicted SOC for all soil types are statistically significant with $p<0.0001$.

Summary statistics calculated on the test data for all relevant soil types indicate the initial model performance across the project's diverse soil conditions:

Soil Type	# Calibration Samples	Test RMSE (wt%)	Test R2
Luvisol	122,570	0.309	0.123
Acrisol	3,610	0.276	0.348
Vertisol	47,575	0.112	0.072
Nitrosol	60,171	0.216	0.095
Cambisol	27,108	0.178	0.156

Complementary to the SOC model, a pedotransfer function (PTF) is developed to estimate bulk density (BD). Recognizing that BD is inversely related to porosity and influenced by soil texture (sand, silt, clay) and SOM, non-linear PTFs are built using the prepared WoSIS dataset. Similar to the SOC model, the WoSIS data is segmented by FAO soil type, and a separate gradient-boosting model (scikit-learn implementation) is trained for each type. These models use sand percentage, silt percentage, and predicted SOC percentage as covariates to predict BD. Hyperparameters were

tuned to minimize test RMSE (e.g., 100 estimators, depth 10). For the Luvisol soil type example, using 555 WoSIS samples split 70-30 for training and testing, the PTF performance is illustrated.

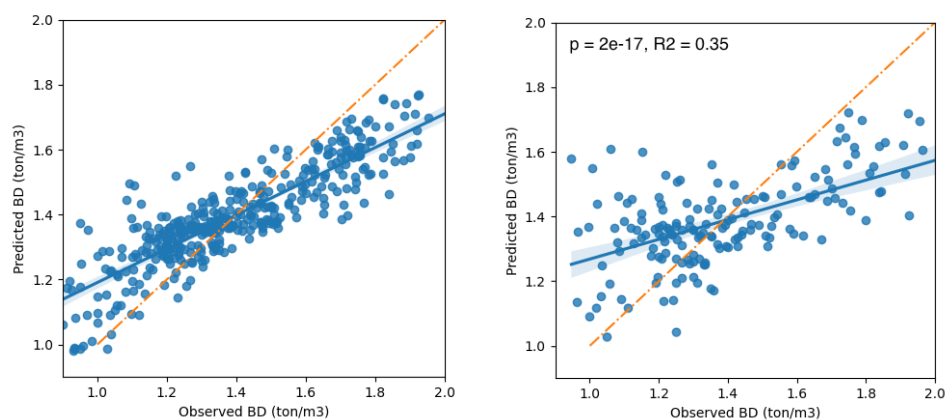


Figure 6. Calibration of the pedotransfer function (PTF) for the determination of BD from SOC, sand and silt percentages in lithisols. The performance on the train data (a) and test data (b) is shown. The graphs are in units ton/m³ (equivalent to g/cm³). There are 388 train data points, and 167 test data points (70-30 train-test split)

The test performance metrics for the BD PTFs across the project's soil types are summarized below:

Soil Type	BD PTF Test RMSE (ton/m ³)	BD PTF Test R2
Luvisol	0.214	0.353
Cambisol	0.193	0.411
Acrisol	0.177	0.563
Vertisol	0.184	0.432
Nitrosol	0.251	0.469

By combining the remote sensing derived SOC (wt%) and the remote sensing & PTF-derived BD (ton/m³), the final soil carbon stock (ton CO₂e/ha) can be calculated for each pixel within the project area.

2.6 Model Validation Metrics

The ongoing validation process provides a continuous check on the model's performance under real project conditions. Before calculating the validation metrics, the new validation samples are incorporated into the modeling process through a leave-one-out simple linear fine-tuning of the initially trained remote sensing ML model output (i.e. a model of the form $a + b * SOC$ to correct the model output for soil data harmonization between the calibration data distribution and the validation lab measurements). This final step ensures that the results are more comparable to the validation

sampling and testing. The model outputs are then compared against the lab measurements from the validation samples to compute key performance indicators including RMSE, R^2 , bias (assessed via t-test for significance at the 5% level), and the 90% Prediction Interval Coverage Probability (PICP) test, which indicates the percentage of validation samples whose actual values fall within the model's 90% prediction interval. These validation metrics were chosen following consultation with remote sensing and soil experts convened by Verra, as part of the registry-led project review of the registration of our Verra projects – these same requirements have been carried over to this Social Carbon project.

The comparison for Luvisols (N=35 farms) is given below:

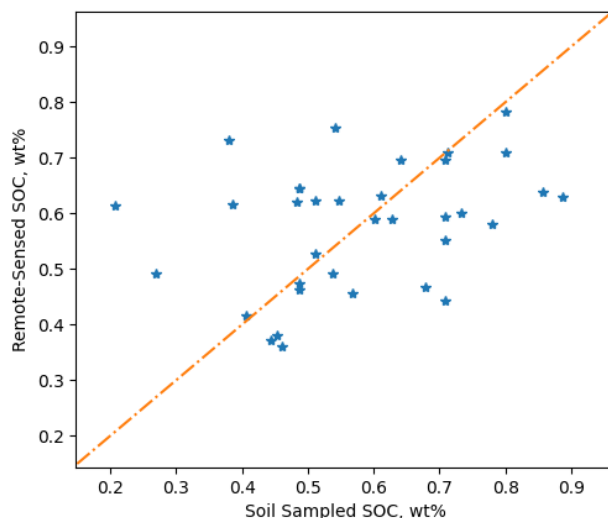


Figure 7. Remote Sensed vs Sampled SOC for the Luvisol validation set

Across all the soil types:

Soil Type	Validation RMSE (ton C/ha)	Validation R2	Bias Significance (5% t-test)	90% PICP (%)
Luvisol	5.3	0.113	5E-4 (not significant)	91
Acrisol	6.3	0.110	4E-4 (not significant)	90
Vertisol	5.7	0.091	2E-5 (not significant)	93
Nitisol	5.0	0.083	3E-6 (not significant)	92
Cambisol	7.6	0.121	9E-4 (not significant)	91

Note that the prediction interval in the PICP is calculated using the uncertainty propagation techniques described in the next section, and thus passing the PICP test is a validation of the uncertainty calculation method as well.

These metric calculations and checks are repeated with each new set of validation samples collected throughout the project's lifetime, ensuring the continued appropriateness of the model and its associated uncertainty quantification.

Are these metrics good enough, when prediction errors are propagated to the project-level? This is answered in the next section.

Section 3: Uncertainty Quantification

3.1 Sources of Uncertainty

Achieving accurate quantification of soil carbon changes necessitates a comprehensive and rigorous assessment of uncertainty from all potential sources. The remote sensing methodology employed, while powerful, carries different types of uncertainty compared to traditional soil sampling. Conventional methods, even with precise lab analysis like dry combustion (individual sample uncertainty $\sim 0.02\text{wt}\%$ ²⁷), face significant uncertainty when scaling up to field or project levels due to sampling error – the error introduced by measuring only a small fraction of the total area. Reaching a high level of observability (e.g., detecting a $0.01\text{wt}\%$ change) with conventional sampling might require hundreds of samples per field. Remote sensing, by measuring every pixel (e.g., $10\text{m} \times 10\text{m}$) across the entire project area, effectively reduces this specific type of sampling error but introduces other uncertainties related to the measurement and modeling process itself.

The uncertainty associated with the remote sensing model outputs arises from several key sources²⁸:

1. **Noise in the input data** (raw satellite data), which is a form of random error
2. **Model Imperfection**: Random error in the model weights, arising during training of the model, and systematic errors wherein the model is unable to capture certain characteristics of the underlying soil carbon variation. Model imperfection can stem from the chosen machine learning architecture, the training process, inherent errors in the training data SOC targets (e.g., $\sim 0.10\text{wt}\%$ uncertainty associated with the Walkley-Black method), unknown variations in ground sample collection procedures, and pre-processing steps like spatialization – matching point-based soil samples to pixel-based satellite data.
3. Potentially incomplete **coverage of the domain** of soil carbon levels in the calibration data. This is minimized by using extensive, representative datasets like the Soil Health Card in India and verifying coverage across relevant soil types, climate zones, and SOC ranges as done in the section above.

In addition, there are 2 types of correlations to be accounted when pixel-level results are aggregated to the farm-level and project-level

- **Spatial Correlations**²⁸: Pixels that are closer to each other are likely to have higher correlation in soil carbon stocks and the input satellite data than pixels that are farther away from each other. Nearby pixels are not independent.
- **Temporal Correlations**: For a given pixel, the absolute soil carbon stocks at each subsequent measurement are expected to be correlated across time, because expected

stock changes are small relative to the absolute level (for example, if SOC starts at 1%, it is expected to remain in the 0.9%-1.1% range over the next 5 years²⁹). Measurements of the same pixel across time are not independent.

Failing to account for these correlations, particularly the degree of spatial correlation when averaging, can lead to an underestimation or overestimation of the true uncertainty at the aggregated level. This effect is well-established in the geostatistics literature. The figure below graphically demonstrates this effect:

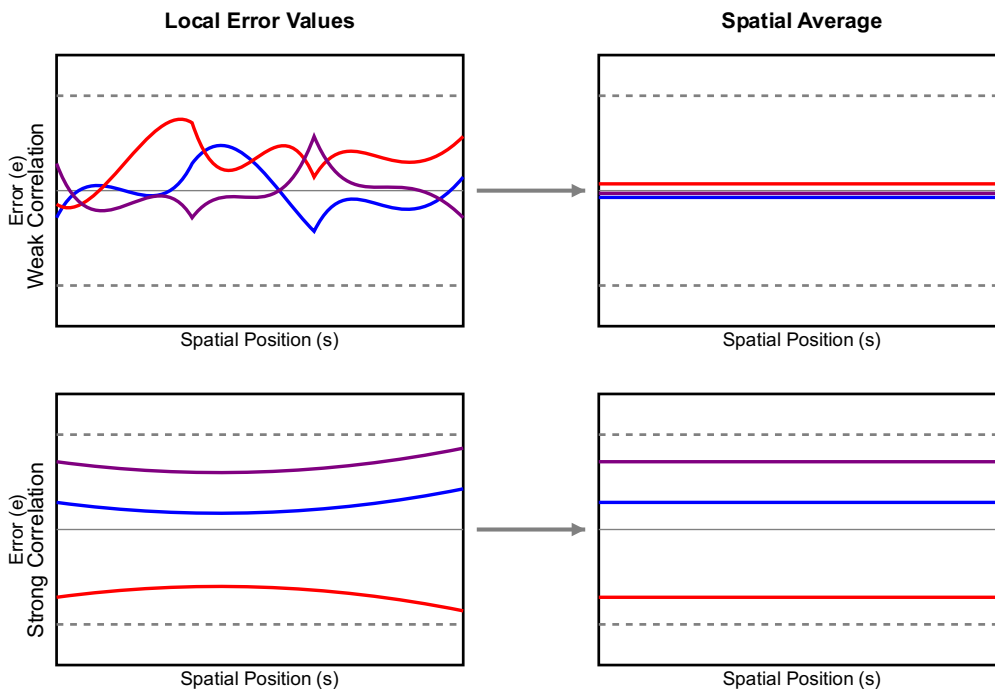


Figure 8. The effect of spatial correlation on the spatial average – weaker correlation leads to lower uncertainty in the spatial average. In the presence of strong spatial correlation, each sample contributes less independent information, limiting the reduction in uncertainty typically achieved through averaging. Therefore, accounting for spatial correlation is essential to avoid overestimating confidence in aggregated values.

A related challenge is model drift over time, where the relationships learned during calibration may become less accurate. This could manifest as label drift (changes in the range of SOC values beyond the calibration set, deemed unlikely for the range of carbon in the farms of this project), covariate drift (changes in satellite sensor characteristics, mitigated by using normalized data products), or concept drift (fundamental changes in the relationship between satellite signals and soil properties). Concept drift might arise from broad systemic changes (e.g., due to climate change effects on soil moisture, minimized by strategic measurement timing; or major policy shifts altering land use, which are monitored) or potentially from the project activities themselves, although the practices promoted are not expected to cause unexpected changes in soil structure beyond those correlated with SOC. Ongoing validation sampling serves as a crucial check for potential model drift.

3.2 Bayesian Approach to Uncertainty Quantification

To comprehensively address these uncertainty sources and correlations, the project employs a Bayesian Monte Carlo approach, specifically utilizing Bayesian Regression Kriging³⁰, a technique well-suited for quantifying map errors holistically. This involves running multiple simulations (e.g., 100) to generate a posterior predictive distribution (PPD) for the SOC stock at each pixel. In each simulation, the ML model is retrained on a random subset (e.g., 70%) of the calibration data, capturing uncertainty in model parameters arising from input noise and model imperfection. A variogram is fitted to the residuals of this model subset to characterize spatially correlated systematic errors, and a simulated residual based on this variogram is added to each pixel's prediction. The collection of results across all simulations forms the pixel-level PPD.

These pixel-level PPDs are then averaged within each farm boundary to produce a farm-level PPD, a process that inherently accounts for the spatial correlations between pixels within the farm. To determine the uncertainty of the change in SOC stock over a monitoring period, the farm-level PPD from the start date of the monitoring period is differenced from the farm-level PPD at the end date. This differencing operation correctly accounts for temporal correlations between the measurements. The resulting distribution is the farm-level SOC Stock Change PPD. The mean of this Change PPD provides the best estimate of the farm's SOC stock change over the period, while the variance (or standard deviation) of this distribution quantifies the standard error associated with that estimate, taking into account input errors, model imperfections, spatial correlations within the farm and temporal correlations across the monitoring period. Figure 8 summarizes the full uncertainty process for a farm:

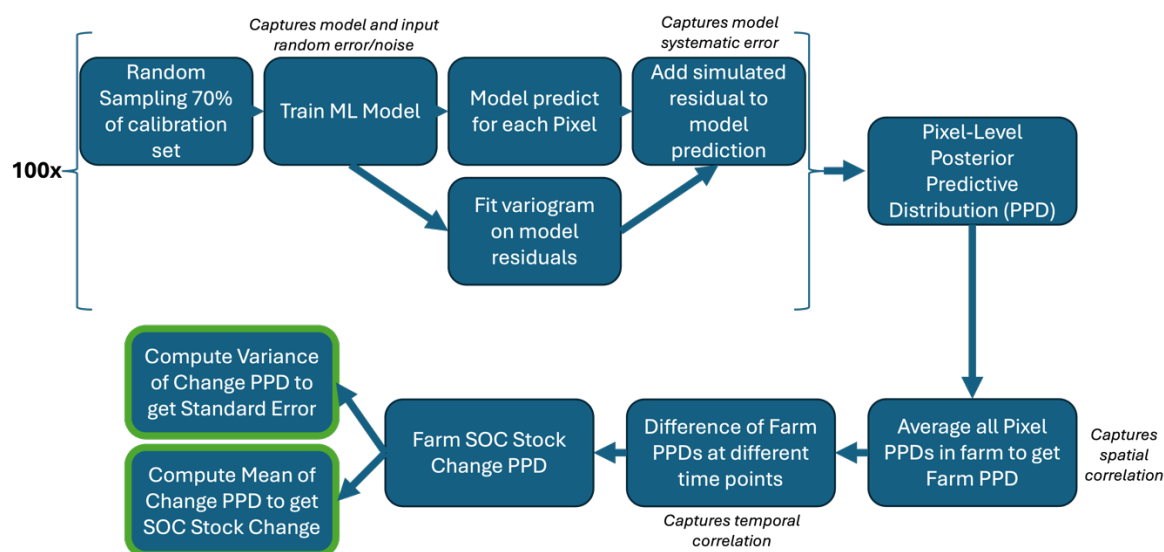


Figure 9. The full process associated with the Bayesian Regression Kriging uncertainty propagation for the soil carbon stock measurement through remote sensing in the India project.

An example calculation for a typical 1.5 ha project farm in Karnataka implementing common practices illustrates this process, with N=100 simulations and 70% sampling in each simulation. The resulting farm-level PPDs for SOC stock each year and the Change PPD for the 2021-2024 period are shown as boxplots:

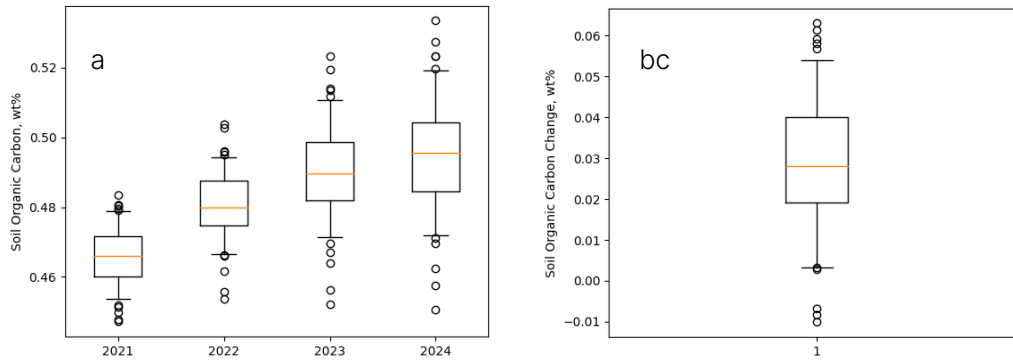


Figure 10. Example farm-level soil carbon Predictive Posterior Distributions (PPDs) from 2021 to 2024 in boxplots (top, a) and the soil carbon change PPD from 2021 to 2024 as a boxplot (bottom left, b). The whiskers in the boxplot represent the 5th and 95th percentile, which are used to show whether the results are significant at a 5% significance level.

For this example farm, the standard deviation of the 3-year SOC stock change was found to be 2.0 ton CO₂e/ha. This translates to a minimum detectable difference (MDD) or prediction interval width of approximately 3.2 to 3.6 ton CO₂e/ha at a 5% significance level.

Importantly, achieving statistical significance for the project overall does not require every individual farm's change to exceed its specific MDD, but rather for the overall project's change to do so. To determine the total project uncertainty, the farm-level Change PPDs are aggregated by area-weighted averaging across all participating farms. This aggregation directly incorporates the spatial covariance between different farms, ensuring a robust estimate of the overall project-level uncertainty. The variance of the final project-level PPD reflects the effects of these inter-farm spatial covariances.

Section 4: Quantification of Net Carbon Removals

The quantification of carbon removals for this project adheres to the SCM0005 V2.0 methodology, specifically employing Quantification Approach 2. This approach is characterized as a 'measure and remeasure' strategy, where SOC stocks are determined at different points in time. SOC stocks at these time points are quantified using Boomitra's remote sensing technology, as detailed in the previous sections, and the remaining steps follow equations in the methodology.

The net carbon removals from the project are calculated using the following equation:

$$NER_y = (TER_y \times (1 - UNC_y)) - PE_y - LE_y$$

Where

- NER_y Net Emission Removals in year *y*; tCO₂e
- TER_y Total project GHG removals in year *y*; tCO₂e
- UNC_y Total uncertainty in project GHG removals in year *y*; percent

PE_y Total project GHG emissions in year *y*; tCO_{2e}

LE_y Leakage of emissions associated with the project in year *y*; tCO_{2e}

The project-level SOC stock change, derived at the end of the previous section, is prorated by day to each year within the monitoring period, to determine TER_y.

Project emissions (PE_y) arising from the implementation of project activities themselves are currently considered negligible for this project (see a more detailed analysis in the full project design document (PDD)). However, should any activities lead to quantifiable emissions during implementation or monitoring, these would be reported in subsequent monitoring cycles.

Leakage (LE_y), representing emissions occurring outside the project boundary due to project activities, is assumed to be zero. This assumption is justified based on the SCM0005 methodology criteria: the project does not involve the application of new manure sourced from outside the project area, and significant productivity declines (greater than 5%) are not anticipated based on literature and project design. Crop productivity will be monitored every ten years as required, and if declines exceeding 5% attributable to project activities are observed (after excluding initial adjustment years if necessary), leakage calculations would be performed according to the methodology. Furthermore, surveys and regional studies indicate that the diversion of biomass like crop residue for soil incorporation under the project does not lead to increased use of non-renewable biomass (e.g., firewood) for other purposes like cooking, as most households in the project region have transitioned to cleaner energy sources such as LPG or improved cookstoves.

An essential component of the net removal calculation is the uncertainty deduction (UNC_y). This deduction accounts for the statistical uncertainty associated with the estimate of total project removals. Following quantification approach 2, the uncertainty arises primarily from the measurement error associated with determining the SOC stock change. This project utilizes the variance derived from the aggregated Posterior Predictive Distributions (PPDs) for SOC stock change to quantify this uncertainty, as described in the previous section. The relative uncertainty is calculated, and a deduction is applied only if this value exceeds a 15% threshold. The formula for the uncertainty deduction is:

$$UNC_y = \text{MIN} \left(100\%, \text{MAX} \left(0, \frac{T \sqrt{\left(S^2_{\Delta SOC_y} + S^2_{\Delta tree_y} + S^2_{\Delta shrub_y} \right)}}{\overline{\Delta CO2_y}} - 15\% \right) \right)$$

Where

UNC_y Total uncertainty; percent

T Critical value of a student's t-distribution for significance level $\alpha = 0.05$ (i.e., a $1 - \alpha = 95\%$ confidence interval) and the degrees of freedom *df* appropriate for the design used (e.g., $df = n - 1$ for a simple random sample of *n* sample units)

$\overline{\Delta CO2_y}$ Areal average carbon dioxide emission removals in year *y*, as determined in the previous section; t CO_{2e}/unit area

- $S^2_{\Delta SOC_y}$ Variance of the estimate of mean emission removals from Soil in year y , as determined through the Bayesian approach in the previous section; (tCO₂e/unit area)²
- $S^2_{\Delta tree_y}$ Variance of the estimate of mean emission removals from Trees in year y ; (tCO₂e/unit area)²
- $S^2_{\Delta shrub_y}$ Variance of the estimate of mean emission removals from Shrubs in year y ; (tCO₂e/unit area)²
- 15% Threshold beyond which there is an uncertainty deduction

In this project, there are no activities leading to tree/shrub planting or removal, so those terms are not used (they are zero).

On the scale of the real project, the farm-level carbon removal between the 2021 and 2024 (the first monitoring period) shows an approximate range from 0 to 4.5, with the density of the distribution declining as carbon removal increases (which is expected):

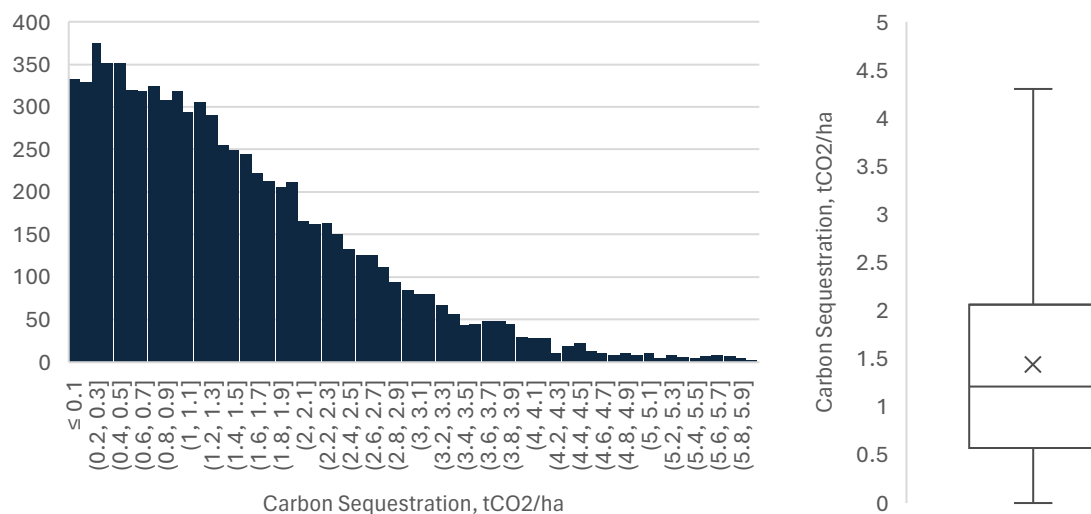


Figure 11. Distribution of carbon sequestration across the farms in the project, as a histogram (left) and boxplot (right).

Similarly, the standard error in carbon removal (standard deviation of the farm stock change PPD) exhibits most of its range between 0.2 and 3:

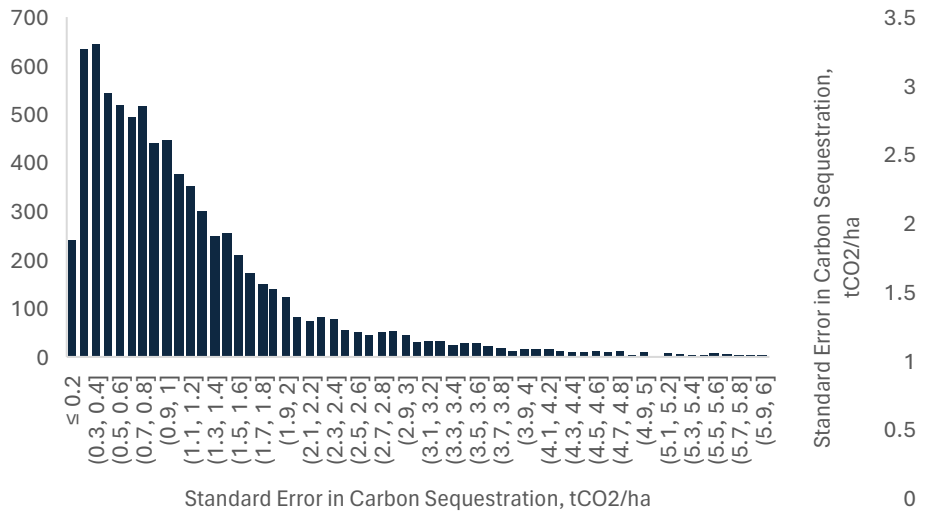


Figure 12. Distribution of the standard error in carbon sequestration across the farms in the project, as a histogram (left) and boxplot (right).

The farm-level numbers are available from the project's registry listing. When aggregated to the project level, through the processes and equations of the last section and this section, this project shows a project-level standard error of 0.0379 ton CO₂e/ha, and a cumulative carbon removal of 52,570 ton CO₂e in the first monitoring period (47,311 ton CO₂e after deducting buffer). These final calculations are also available in the registry listing.

Section 5: Discussion and Limitations

5.1 Interpreting the Sequestration Results in Context

The observed mean soil carbon sequestration rate during the initial monitoring period (2021–2024) was approximately 0.5 tC/ha/year (1.7 tCO₂e/ha/year or 0.01 wt%/year) across participating farms. This aligns with global literature for similar regenerative agriculture practices. Multiple meta-analyses place sequestration potential from interventions such as residue incorporation, organic fertilizer use, and cover cropping in the range of 0.2–0.7 tC/ha/year (0.7–2.6 tCO₂e/ha/year or 0.004–0.014 wt%/year).³¹

Figure 12 illustrates these ranges across various management practices (e.g., no-till vs. tillage intensity, cover cropping, composting) and climate zones. Green bars indicate tropical regions like those in this project.

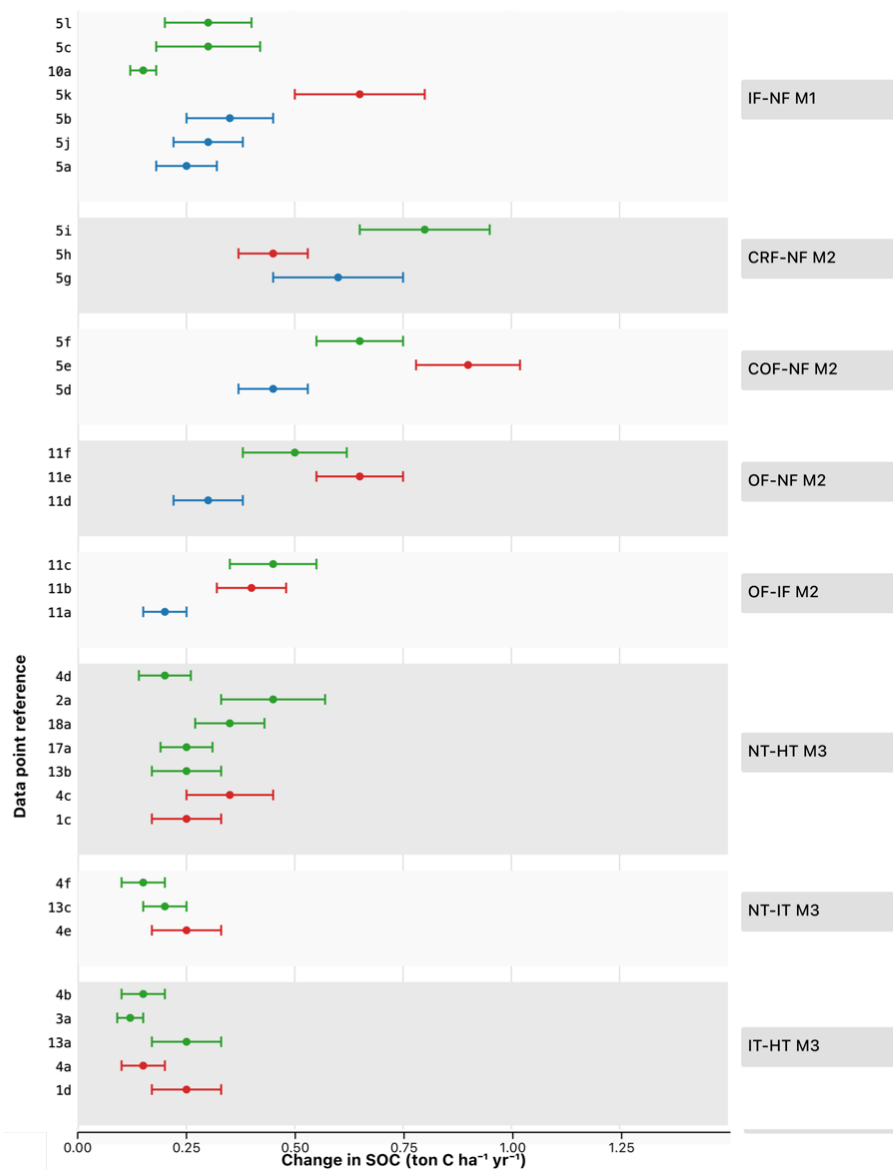


Figure 13. Meta-analysis of sequestration rates across several improved agricultural management studies. Green represents tropical climates, red subtropical, and blue temperate. Management practices: Inorganic fertilizer - no fertilizer (IF-NF); Increased organic matter input (M2): Combined fertilizer relative to No Fertilizer (COF-NF), Combined Straw +fertilizer relative to No Fertilizer (CRF-NF), Organic Fertilizer relative to Inorganic Fertilizer (OF-IF), Organic Fertilizer relative to No Fertilizer (OF-NF); Decreased tillage (M3): No-Till relative to High Intensity-Till (NT-HT), No-Till relative to Intermediate Intensity-Till (NT-IT) and Intermediate Intensity-Till relative to High Intensity-Till (IT-HT); Increased crop diversity (M4): Crop rotation +cover crops (CC) and perennial crop rotation (CCP); Crop residue incorporation (M5): crop residue incorporation vs. removal (CRES). Adapted from Lessman et al.³¹

This project's rates fall within these expected ranges. Importantly, the sequestration rate is expected to decrease over time as soils reach a new equilibrium, unless additional practices are introduced. This trajectory reflects natural saturation dynamics of soil carbon systems.

5.2 Model Strengths and Practical Value

The remote sensing MRV system used in this project offers major advantages over traditional approaches:

- **Significant Cost Reduction:** Traditional approaches would require sampling each of the 8,000+ smallholder farms. This project instead utilizes a few hundred well-distributed samples for validation, reducing costs dramatically while maintaining scientific integrity.
- **Improved Sampling Quality:** By requiring fewer samples overall, we are able to deploy a small team of highly trained field technicians and work exclusively with trusted laboratories, ensuring scientific accuracy and rapid turnaround times. Soil sampling is a precise science—if a much larger volume of samples were needed in a short timeframe, it would be infeasible to rely on expert teams alone. That would introduce greater risk of error from less experienced personnel and inter-lab variability, both of which are common challenges in traditional soil carbon testing.
- **Reproducibility and Transparency:** The system's reliance on publicly available satellite images and consistent machine learning models ensures reproducible outputs. Any third party could repeat the process using the same input data and model to yield identical SOC estimates.
- **Audit-Ready and Registry-Consistent:** The system meets the technical requirements for both the Social Carbon standard and overlapping expectations from Verra's VCS. Validation results include RMSE, R^2 , bias testing (t-test), and prediction interval coverage probability (PICP), each updated with every verification cycle.

5.3 Limitations and Considerations

While the methodology is robust within its design parameters, several important limitations must be acknowledged:

- **Regional Calibration:** The model is developed specifically for Indian cropping systems and soil types. Application outside these areas would require recalibration with local datasets and soil validation.
- **Bulk Density (BD) Estimation Constraints:** The BD pedotransfer function assumes relatively stable soil compaction history or changes that are tightly correlated with SOC. This assumption may not hold immediately following a transition to no-till agriculture, where bulk density can increase temporarily in ways not directly related to SOC. Although this limitation is specific to no-till systems, which are not promoted within the URVARA project, it's important to clarify that some international readers may expect to see no-till included due to its popularity in the U.S. and Europe. However, no-till is generally avoided in this project context because it often increases weed pressure, which can lead to greater reliance on herbicides—conflicting with the organic principles followed by many of our implementation partners.
- **Decadal and Climate-Driven Soil Changes:** Over 30–100 year timescales, broader shifts such as erosion, climate-induced changes to moisture regimes, or altered cropping patterns could affect the validity of initial calibration. This is mitigated through ongoing validation and the requirement for a full baseline reassessment every 10 years.

5.4 Robustness in Reversal Monitoring

One of the most impactful benefits of remote sensing is its ability to continuously monitor all farms in the project—even after an individual farmer exits. Conventional soil-sampling-based projects often assume a 100% reversal (i.e., total loss of credited carbon) if the farmer leaves the project, due to the inability to revisit or resample the site. In contrast, Boomitra's system enables continued SOC measurement through remote sensing, allowing any actual loss to be measured and accounted for without defaulting to total forfeiture.

This approach provides a major advantage in terms of permanence and reversal monitoring and is particularly crucial for building large-scale soil carbon projects with a 100+ year permanence guarantee..

5.5 Advantages of Ex-Post Credit Issuance

This project issues carbon credits **exclusively on an ex-post basis**, i.e., only after SOC changes are measured through both remote sensing and ground validation. This sharply contrasts with many projects that rely on **ex-ante credit issuance** where credits are generated in advance based on future projections without measurement-based confirmation.

Key differences:

- **Ex-Post (This Project):** Credits are issued only after SOC changes are directly measured and verified during each monitoring period. While machine learning models are used in this process, they operate only within the context of observed satellite data and calibrated relationships that are validated with ground truth for each measurement timepoint. These are not forward projections across time, and credits are never issued based on modeled outputs alone.
- **Ex-Ante (Not Used Here):** Several projects commonly issue credits based on predicted SOC increases before any measurement takes place. The credits are later adjusted ('true-upped') when new data is available, leading to possible over-crediting or under-crediting in the interim. This project avoids such practices entirely, reinforcing confidence in the resulting credits.

Boomitra's conservative, measurement-based, ex-post approach enhances credibility with credit buyers and aligns more closely with emerging standards for high-integrity carbon removal.

5.6 Remote Sensing for High-Quality, Scalable MRV

The remote sensing model employed here addresses many challenges faced by soil carbon projects:

- It reduces per-farm MRV cost to enable participation by smallholders.
- It increases temporal resolution and reliability of data.
- It ensures that credits reflect real, measurable carbon removal.

Moreover, it builds resilience into the project design—capable of adjusting to changing field conditions, verifying ongoing performance, and supporting robust credit issuance throughout the multi-decade lifecycle of a soil carbon project.

Remote sensing has the potential to solve many of the challenges that soil carbon projects face today, from monitoring reliability to cost. Boomitra is proud to lead the way in bringing this technology to farms of all sizes around the world.

Appendix A: Reader Questions and Responses

We invite you to submit comments and questions on this work using [this form](#). All submissions will be reviewed and addressed, and this appendix will be updated regularly with submitted questions and comprehensive author responses.

¹ Lessmann, M., Ros, G. H., Young, M. D., & de Vries, W. (2022). Global variation in soil carbon sequestration potential through improved cropland management. *Global Change Biology*, 28, 1162–1177. <https://doi.org/10.1111/gcb.15954>

² S&P Platts CRC (Carbon Removal Credit) pricing index: <https://cilive.com/commodities/energy-transition/news-and-insight/090624-interactive-platts-carbon-price-explorer>

³ SERVIR GLOBAL. (2019). *SAR Handbook: Comprehensive methodologies for forest monitoring and biomass estimation*. <https://ntrs.nasa.gov/api/citations/20190002563/downloads/20190002563.pdf>

⁴ Babaeian, E. *et al.* (2019) 'Ground, proximal, and satellite remote sensing of soil moisture', *Reviews of Geophysics*, 57(2), pp. 530–616. doi:10.1029/2018rg000618.

⁵ Roth, K. *et al.* (1990) 'Calibration of time domain reflectometry for water content measurement using a composite dielectric approach', *Water Resources Research*, 26(10), pp. 2267–2273. doi:10.1029/wr026i010p02267.

⁶ Shimobe, S., & Spagnoli, G. (2018). Relationship between dielectric constant of soils with clay content and dry unit weight. *Environmental Geotechnics*, 8(2), 134–147.

⁷ Malicki, M. A., Plagge, R., & Roth, C. H. (1996). Improving the calibration of dielectric TDR soil moisture determination taking into account the solid soil. *European Journal of Soil Science*, 47(3), 357–366.

⁸ Y. Gao *et al.*, "Evaluation of the Tau–Omega Model for Passive Microwave Soil Moisture Retrieval Using SMAPEX Datasets," in *IEEE Journal of Selected Topics in Applied Earth Observations and Remote Sensing*, vol. 11, no. 3, pp. 888–895, March 2018, doi: 10.1109/JSTARS.2018.2796546.

⁹ de Rosnay, P., Rodriguez-Fernandez, N., Muñoz-Sabater, J., Albergel, C., Fairbairn, D., Lawrence, H., ... & Kerr, Y. (2018, July). SMOS data assimilation for numerical weather prediction. In *IGARSS 2018-2018 IEEE International Geoscience and Remote Sensing Symposium* (pp. 1447–1450). IEEE.

¹⁰ Bahrami, H., McNairn, H., Mahdianpari, M., & Homayouni, S. (2022). A meta-analysis of remote sensing technologies and methodologies for crop characterization. *Remote Sensing*, 14(22), 5633.

¹¹ Van Looy, K. *et al.* (2017) 'Pedotransfer functions in Earth System Science: Challenges and perspectives', *Reviews of Geophysics*, 55(4), pp. 1199–1256. doi:10.1002/2017rg000581.

¹² Indian Census Data, as quoted in CEIC Data: <https://www.ceicdata.com/en/india/agriculture-census-average-size-of-operational-land-holdings-by-size-group/agriculture-census-average-size-of-operational-land-holdings-size-group-all-holdings>

-
- ¹³ Dimri, A. P., Yasunari, T., Kotlia, B. S., Mohanty, U. C., & Sikka, D. R. (2016). Indian winter monsoon: Present and past. *Earth-science reviews*, *163*, 297-322.
- ¹⁴ A widely reported statistics quoted by NITI Aayog - <https://www.livemint.com/news/india/over-50-of-india-s-cultivated-land-now-has-assured-irrigation-thanks-to-expansion-in-micro-projects-and-efficient-water-use-11685555001532.html>
- ¹⁵ <https://www.india.gov.in/spotlight/soil-health-card>
- ¹⁶ Sahrawat, K. L. Carbon Status of Indian Soils: An Overview.
- ¹⁷ Batjes, N. H., Ribeiro, E., Van Oostrum, A., Leenaars, J., Hengl, T., & Mendes de Jesus, J. (2017). WoSIS: providing standardised soil profile data for the world. *Earth System Science Data*, *9*(1), 1-14.
- ¹⁸ Intergovernmental Panel on Climate Change (IPCC). (2019). 2019 Refinement to the 2006 IPCC guidelines for national greenhouse gas inventories. *Agriculture, forestry and other land use*, *4*, 824.
- ¹⁹ Nachtergaele, F., van Velthuisen, H., Verelst, L., Wiberg, D., Henry, M., Chiozza, F., ... & Tramberend, S. (2023). *Harmonized world soil database version 2.0*. FAO.
- ²⁰ FAO GLOSOLAN is a global program for harmonizing measurements across laboratories, and thereby increasing the consistency of worldwide soil testing. Learn more here: <https://www.fao.org/global-soil-partnership/glosolan/en/>
- ²¹ <https://sentiwiki.copernicus.eu/web/s2-processing#S2Processing-CopernicusSentinel-2Collection-1AvailabilityStatus>
- ²² https://www.eorc.jaxa.jp/ALOS/en/index_e.htm
- ²³ https://www.eorc.jaxa.jp/ALOS/en/dataset/fnf_e.htm
- ²⁴ <https://smap.jpl.nasa.gov/>
- ²⁵ Copernicus Climate Change Service, Climate Data Store, (2018): Soil moisture gridded data from 1978 to present. Copernicus Climate Change Service (C3S) Climate Data Store (CDS). DOI: [10.24381/cds.d7782f18](https://doi.org/10.24381/cds.d7782f18)
- ²⁶ <https://documentation.dataspace.copernicus.eu/Data/ComplementaryData/SMOS.html>
- ²⁷ <https://anlab.ucdavis.edu/analysis/Soils/322>
- ²⁸ Wadoux, A.M. and Heuvelink, G.B. (2023) 'Uncertainty of spatial averages and totals of natural resource maps', *Methods in Ecology and Evolution*, *14*(5), pp. 1320–1332. doi:10.1111/2041-210x.14106.
- ²⁹ Poeplau, C., Gregorich, E. (2022). Advances in measuring soil organic carbon stocks and dynamics at the Profile Scale. *Burleigh Dodds Series in Agricultural Science*, 323–350. <https://doi.org/10.19103/as.2022.0106.10>
- ³⁰ Banerjee, S., Carlin, B. P., & Gelfand, A. E. (2003). *Hierarchical modeling and analysis for spatial data*. Chapman and Hall/CRC.
- ³¹ Lessmann, M., Ros, G. H., Young, M. D., & de Vries, W. (2022). Global variation in soil carbon sequestration potential through improved cropland management. *Global Change Biology*, *28*, 1162–1177. <https://doi.org/10.1111/gcb.15954>